JOURNAL OF MATERIALS SCIENCE 5 (1970) 127-132

The Effect of Particle Size upon the Annealing Behaviour of Plastically Deformed Two-Phase Crystals

T. C. ROLLASON, J. W. MARTIN
Department of Metallurgy, The University, Oxford, UK

Two-phase crystals of copper containing dispersed SiO_2 particles and of aluminium containing plates of $CuAl_2$ (θ-phase) have been prepared and plastically deformed at room temperature. The changes in dislocation distribution upon isothermal annealing have been followed by electron microscopy.

It is shown that misoriented subgrains associated with the dispersed phase form on annealing only if the dislocation interactions during prior straining lead to the development of local lattice curvature in the matrix at these regions. When the dispersed particle size is small (i.e. < 3000 Å in diameter) no such recrystallisation embryos are observed, and a microstructure which should provide optimum resistance to recrystallisation is suggested.

1. Introduction

Many high-strength alloys have a microstructure consisting of a matrix containing a high density of dislocations and a dispersed finely-divided second phase, and for strength at high temperatures the dispersed phase must retard recovery and recrystallisation of the matrix, thus maintaining a high dislocation density. Experiments have been carried out in this laboratory on aluminium containing various dispersions of θ ($CuAl_2$)-phase in both single and polycrystals [1, 2], and on copper single crystals containing dispersions of SiO_2 [3] and cobalt particles [4]: the changes in properties and microstructure upon isothermal annealing of the cold-worked alloys were followed so that the effectiveness of the dispersed phase in retaining a high dislocation density could be assessed.

It is found that the dispersed phase can either accelerate or retard recrystallisation, compared to the behaviour of the (precipitate-free) matrix, and that the important factor appears to be the interparticle spacing. The effect can be explained in general terms by considering that the precipitate will have the effect of increasing the dislocation density when the specimen is plastically deformed, thus increasing the driving force for recrystallisation. A precipitate impedes the motion of grain-boundaries, however, and the observed behaviour may be ascribed to the former effect predominating at large interparticle spacings and the latter at small interparticle spacings. This kind of explanation takes no account of the dislocation configurations in the system, and our present work has been aimed at clarifying part of this aspect.

When a crystal containing hard inclusions is subjected to plastic deformation, "geometrically necessary" dislocations are formed at the particles to solve the compatibility problem which arises because the inclusions remain undeformed when the specimen as a whole deforms. Ashby [5] has pointed out that these "compatibility" dislocations could either form as secondary glide loops, which would involve local *lattice bending* adjacent to each particle, or exist as prismatic dislocations, which would not involve local curvature of the matrix lattice. From the point of view of recrystallisation resistance, regions of high local lattice curvature adjacent to particles are undesirable as they could readily provide recrystallisation embryos, and our present object has been to investigate this possibility by examining the effect of annealing

for short times upon deformed two-phase crystals containing each type of distribution of geometrically necessary dislocations.

2. Experimental Procedure

2.1. The Production of Two-Phase Crystals

Cylindrical single crystals were grown by a modified Bridgman technique. Two alloy systems were used: aluminium – 5 wt % copper and copper – 0.11 wt % silicon, and crystals were chosen with orientations near the centre of the stereographic triangle. The heat-treatments were as follows:

2.1.1. Aluminium-Copper Alloy

A stable dispersion of the equilibrium θ ($CuAl_2$)-phase was required, so the heat-treatment technique due to Shaw, Shepard, Starr, and Dorn [6] was employed. After a 72 h solution anneal at 540° C followed by water-quenching to room temperature, the alloy was aged 75 sec at 450° C and water-quenched, then aged for a further 1 h at 400° C and subsequently furnace-cooled to 305° C, held at that temperature for 48 h and finally water-quenched to room temperature.

2.1.2. Copper-Silicon Alloy

Internal oxidation was carried out by the method of Rhines *et al* [7] at a temperature of 950° C. In order to minimise particle size variation across the specimen diameter, the outer layers (which contain the greatest variation in particle size) were removed by acid-machining.

2.2. Tensile Deformation

Tensile specimens were prepared by acid-machining of the single crystals, which were finally electropolished. They were deformed at room temperature, all at a strain rate of 2.5×10^{-4} sec^{-1}.

2.3. Annealing Treatment

Sections 1 mm thick were cut from the deformed crystals by spark-machining, and these were then thinned chemically to a thickness of 0.6 mm to remove any damage from the spark-machining.

The samples were then annealed at 305° C (Al-Cu) and 700° C (Cu-SiO_2) in a salt-bath for the times stated below.

2.4. Metallography

All specimens prepared for electron microscopy from tensile specimens were sectioned in known crystallographic directions; the two sections principally examined were those parallel to the primary glide plane (1 1 1), and those normal to this plane and to the primary Burgers vector, i.e. (–1 0 1) sections.

Discs 3 mm in diameter were trepanned by spark-machining from the 1 mm thick sections discussed above, and these were electropolished in a PTFE holder, then mounted in a holder which enabled orthogonal tilts of ± 20° to be

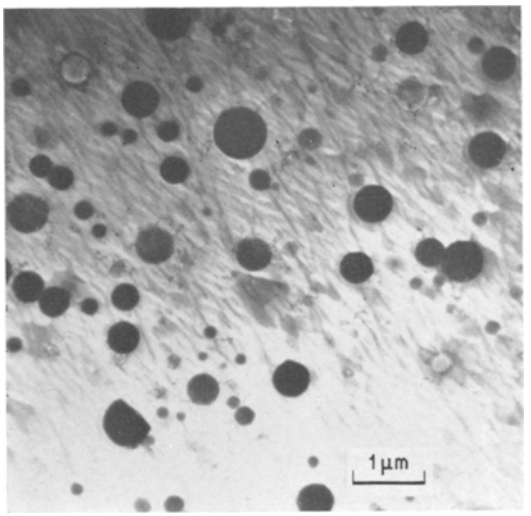

Figure 1 Dispersion of spherical silica particles in copper, produced by internal oxidation of copper-0.11 wt % silicon alloy at 950° C.

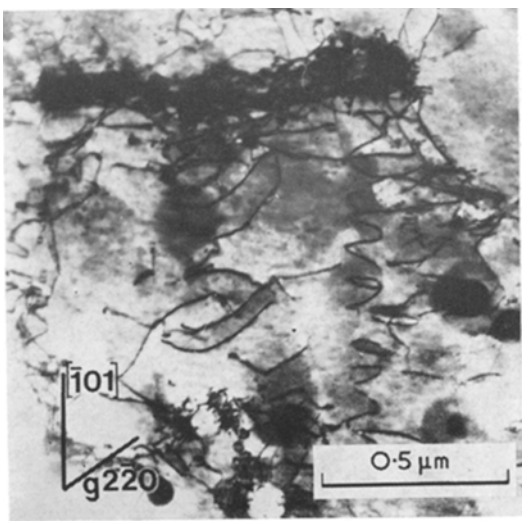

Figure 2 Specimen as in fig. 1 after a shear strain of 20% showing aligned dislocation loops and helices of primary Burgers vector associated with the smaller silica particles. (1 1 1) section.

obtained, and examined in an EM6 electron microscope using 100 kV electrons.

3. Results and Discussion

3.1. Copper-Silica Crystals

After internal oxidation the microstructure of this alloy appeared as shown in fig. 1; it consists of a dispersion of amorphous spheres of silica in copper. The oxide particle size ranged from 1200 to 8000 Å in diameter.

After a tensile deformation to a shear strain of 20%, observation in the electron microscope of thin foil specimens showed that two types of dislocation-particle interactions had occurred, depending upon the size of the silica particle. As shown in the (1 1 1) section of fig. 2, at particle sizes less than approximately 3000 Å diameter, aligned prismatic dislocation loops (shown by contrast experiments to possess the primary Burgers vector) were observed. Their direction of alignment was parallel to the primary Burgers vector; aligned dislocation dipoles and occasional dislocation helices were also present. These observations are in agreement with those of Humphreys and Martin [8], and the origin of the structure may be understood in terms of their explanation, namely by the cross-slip of edge dislocations which, when bowed at a particle under the applied stress, leave prismatic loops adjacent to the particle, and the formation in each dislocation of two large jogs, whose presence can lead to other more complex interactions.

Dislocation interactions with the larger diameter silica particles were more complex, there being no evidence of primary prismatic dislocation loops in the vicinity. The ($\bar{1}$ 0 1) section of fig. 3 illustrates the type of structure observed, first reported by Stobbs and Brown [9], which is characterised by intense secondary slip activity in the matrix adjacent to the particle which gives rise to a local bending or rotation of the lattice. In the micrograph of fig. 3, which was imaged in a $\mathbf{g} = (0\ 2\ 0)$ reflection, the region of intense slip activity adjacent to the large particle is bounded by [1 $\bar{2}$ 1] and [1 2 1] directions. Further contrast analysis has shown that these regions correspond to dislocations on the cross-slip plane. The local rotations, which are of the order of 1°, have been analysed by a microdiffraction technique by Chapman and Stobbs [10], and the senses of the axes of rotation were to be expected from the action of local negative secondary slip.

The two types of dislocation-particle interaction illustrated in figs. 2 and 3 have been discussed by Ashby [5], whose interpretation may be summarised diagrammatically in fig. 4. Fig. 4a shows an element of undeformed crystal containing a hard inclusion of a second phase. In fig. 4b the inclusion has been removed and the crystal sheared uniformly; since the inclusion cannot be deformed, the hole from which it came must be restored to its original shape if the inclusion is to be replaced.

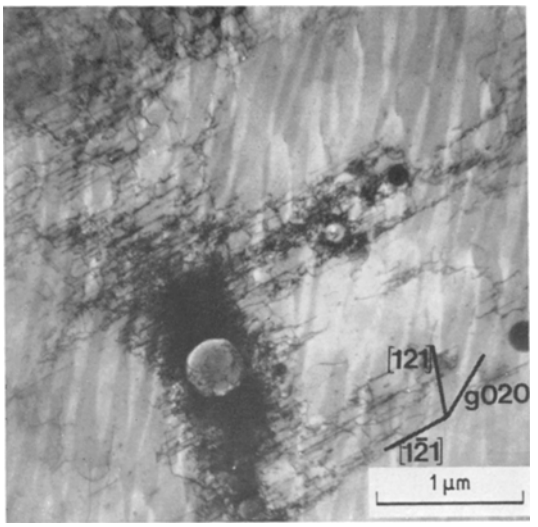

Figure 3 Specimen as in fig. 2 showing intense local secondary slip activity adjacent to a large silica particle. ($\bar{1}$ 0 1) section.

Figs. 4c and d show the hole restored to its original shape by shear dislocation loops on primary and secondary systems respectively. This process leads to local lattice bending of the matrix in these regions, and is a simplification of the type of process which has taken place in the specimen of fig. 3.

Figs. 4e and f show the hole restored to its original shape by prismatic glide, which does not involve bending the matrix lattice. In fig. 4e, loops of primary Burgers vector are formed and the dislocation structure corresponds to that of fig. 2. In fig. 4f, dislocations of secondary Burgers vector are formed, but because they are prismatic loops, their presence would not involve local lattice curvature.

The deformed crystals were annealed at 700° C for short periods, and figs. 5a, b, and c show typical dislocation structures observed after 3 min at this temperature. The annealing response was observed to differ in the regions

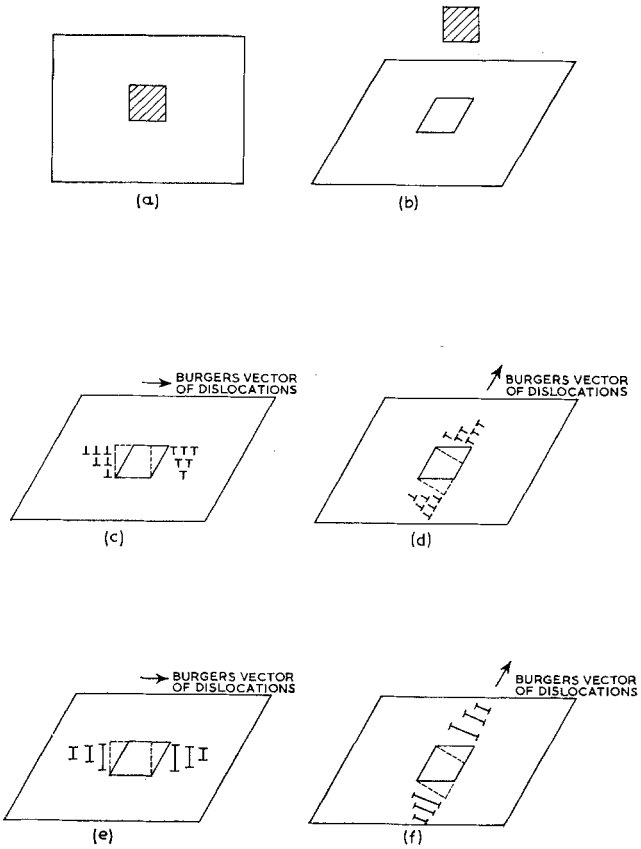

Figure 4 (a) Shows an element of crystal containing a hard inclusion of a second phase (shown prior to deformation) (b) The inclusion has been removed and the crystal sheared uniformly. (c) and (d) Show the hole restored to its original shape by the emission of glide dislocations on (c) the primary system and (d) a secondary system. (e) and (f) Show the hole restored to its original shape by prismatic glide.

adjacent to small and to large silica particles: adjacent to the smaller silica particles (e.g. regions A) a low dislocation density is restored by a process of recovery. This observation is in agreement with those of Humphreys and Martin [4] upon two-phase copper-cobalt alloy crystals containing particles of approximately 800 Å diameter. When these were deformed into Stage I of the stress-strain curve, no recrystallisation was observed, but complete recovery to low dislocation densities was found after annealing at 700° C.

Adjacent to the larger particles (whose as-deformed structure was shown in fig. 3) annealing has given rise to regions of high local misorientation which clearly could provide embryos for the nucleation of recrystallisation of the alloy. Figs. 5a and b are of the same area taken in different reflections, and these illustrate that the misorientation associated with the large particles is complex and can be described in terms of a rotation about several axes. For example, the region of dark contrast, C, in fig. 5a is out of contrast in fig. 5b (when $\mathbf{g} = 1\,\bar{1}\,1$) which suggests a $<1\,0\,1>$-type rotation axis. In fig. 5b the areas of dark contrast are bounded by $[1\,\bar{2}\,1]$ and $[1\,0\,1]$ directions, and comparison with fig. 3 will show that there has been an appreciable sharpening of contrast at the interface between these areas and the rest of the crystal.

Fig. 5c (taken in $\mathbf{g} = 0\,2\,0$) shows an array of closely-spaced straight dislocations (D) in the misoriented region. Contrast experiments suggested that these were of edge character, and they formed a tilt boundary: this configuration might be expected from a polygonisation process.

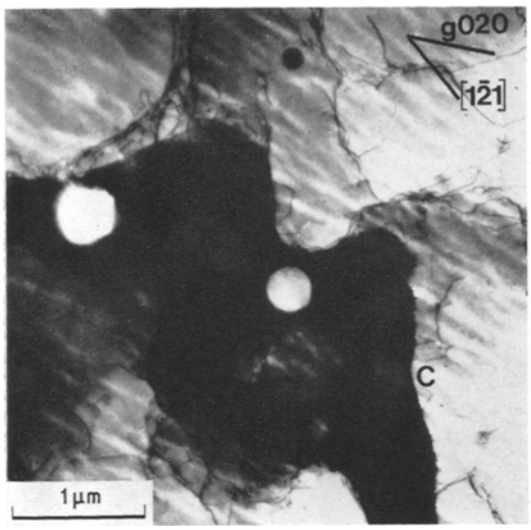

(a)

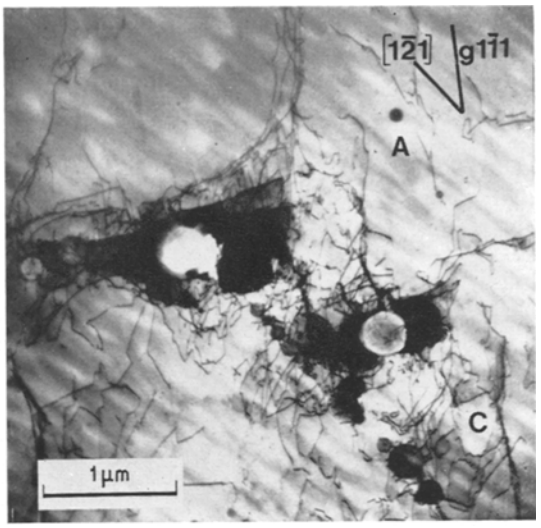

(b)

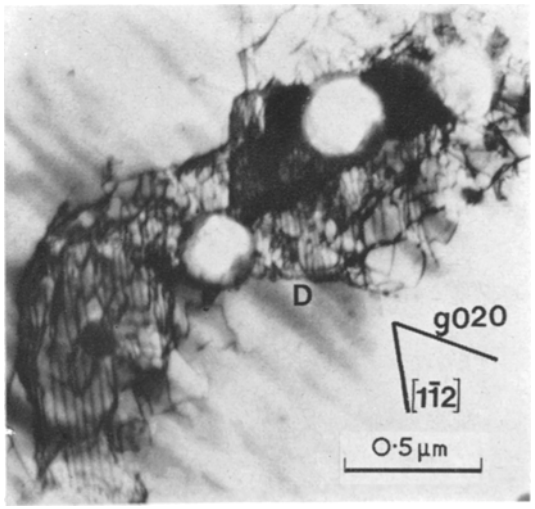

(c)

Figure 5 (a, b and c) Specimen as in fig. 3 after annealing for 3 min at 700° C. ($\bar{1}$ 0 1) section.

3.2. Aluminium-$CuAl_2$ Crystals

After ageing, the microstructure of this alloy consisted of a dispersion of plates of the θ-phase of approximately 500 Å thickness and of diameter ranging from 0.25 to 1.20 μm. After tensile deformation to a shear strain of 10% the microstructure was similar to that reported by Stewart and Martin [11], in that dislocations possessing the primary Burgers vector tended to be in regions remote from the particles. In the immediate vicinity of the θ-plates, however, a high density of secondary dislocations accompanied by local lattice rotation was observed. Such local rotations have also been detected by the presence of Laue asterism in X-ray diffraction [12], and Ashby [5] has pointed out that plates and needles give rise to a more severe compatibility problem than equiaxed inclusions, so that local lattice bending is more likely in this type of two-phase microstructure. Indeed recent work has demonstrated [13] that small, equiaxed particles in aluminium crystals will, upon deformation, give rise to prismatic loops in exactly the same manner as in the two-phase copper crystals discussed in the previous section.

The deformed material was annealed at 305° C, as this was the temperature at which the θ-phase had been stabilised after ageing (so that no reversion or further precipitation would take place during the heat-treatment) and fig. 6 shows the microstructure observed after 1 min at this temperature.

As in the case of the coarse silica particles in copper, it is found that the regions of intense secondary slip activity immediately adjacent to the particles have given rise on annealing to zones of significant misorientation with respect to the rest of the crystal. A network of misoriented regions exists, seen as characteristic dark areas in fig. 6, and they are invariably associated with θ-phase particles (which are themselves aligned along $<1\,0\,0>$ directions). The dislocation density is still high, and this fact, coupled with the absence of subgrains or cells

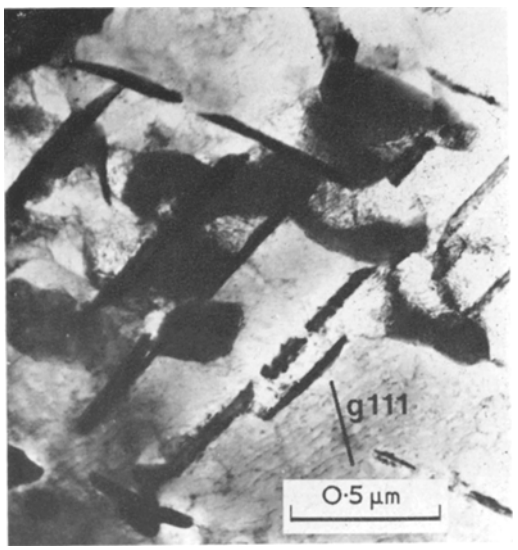

Figure 6 Aluminium-5 wt % copper crystal containing plates of θ ($CuAl_2$)-phase, deformed to a shear strain of 10% and annealed at 305°C for 1 min. ($\bar{1}$ 0 1) section.

and the small diameter of the misoriented regions, meant that no Kikuchi line shift measurements could be made because of the diffuse character of the Kikuchi bands.

4. General Discussion and Conclusions

The present series of experiments has deliberately disregarded the effect that second phase particles have in impeding the motion of grain- (and sub-grain-) boundaries. Our primary concern has been with how the increased dislocation density arising from the presence of the particles in deformed two-phase alloys of this type may influence the nucleation of recrystallisation.

Acceleration of nucleation of recrystallisation in the presence of a second phase has been commonly observed (e.g. [14-19]), and it has been in general qualitatively accounted for on the basis that the cold-work caused increased local lattice curvature adjacent to the second phase particles; but the present work has demonstrated that in both copper-based and aluminium-based alloys this effect is dependent upon the size and shape of the dispersed particles. We may therefore conclude that, for optimum recrystallisation resistance, a hard stable dispersed phase should have a particle diameter below the range 3000 to 5000 Å in order to suppress the development of local lattice curvatures on deformation, and furthermore that equiaxed, rather than plate-like morphologies are preferable [5, 13].

The ability of the recrystallisation embryos observed in the present alloys to act as nuclei for recrystallisation is likely to depend upon the interparticle spacing [1]. Acceleration of recrystallisation due to these effects is generally associated with relatively wide interparticle spacings (e.g. 8 μm [14]), whereas significant retardation due to particle-pinning effects does not appear to become appreciable until the interparticle spacing is of the order of 1 μm or less [1, 3]. The present results suggest, therefore, that the microstructural requirement in recrystallisation-resistant alloys under the conditions investigated here would be the distribution of small, equiaxed particles at interparticle spacings of not more than, say, 1 μm.

Acknowledgement

The authors wish to thank Professor P. B. Hirsch FRS for the laboratory facilities made available and the Ministry of Technology for support.

References

1. R. D. DOHERTY and J. W. MARTIN, *J. Inst. Met.* **91** (1963) 332.
2. *Idem, Trans. ASM* **57** (1964) 874.
3. F. J. HUMPHREYS and J. W. MARTIN, *Acta Met* **14** (1966) 775.
4. *Idem, Phil Mag.* **17** (1968) 365.
5. M. F. ASHBY, Harvard Univ. Tech. Rept. No. 549 (1968).
6. R. B. SHAW, L. A. SHEPARD, L. A. STARR, and J. E. DORN, *Trans. ASM* **45** (1953) 249.
7. F. N. RHINES, W. A. JOHNSON, and W. A. ANDERSON, *Trans. AIME* **147** (1942) 205.
8. F. J. HUMPHREYS and J. W. MARTIN, *Phil Mag.* **16** (1967) 927.
9. W. M. STOBBS and L. M. BROWN, Proc. 4th Eur. Conf. Electron Micr. (Rome) (1968) 413.
10. P. F. CHAPMAN and W. M. STOBBS, *Phil Mag.* **19** (1969) 1015.
11. A. T. STEWART and J. W. MARTIN, Proc. 4th Eur. Conf. Electron Micr. (Rome) (1968) 407.
12. R. J. PRICE and A. KELLY, *Acta Met.* **12** (1964) 159.
13. A. T. STEWART and J. W. MARTIN, unpublished work.
14. J. W. MARTIN, *Metallurgia* **55** (1957) 161.
15. T. LL. RICHARDS and S. F. PUGH, *J. Inst. Met.* **88** (1959) 141.
16. W. M. WILLIAMS and R. EBORALL, *ibid* **81** (1952) 501.
17. V. A. PHILLIPS and A. PHILLIPS, *idem* p. 185.
18. M. K. B. DAY, *Mem. Sci. Rev. Met.* **56** (1959) 201.
19. P. R. MOULD and P. COTTERILL *J. Mater. Sci.* **2.** (1967) 241

Received 15 September and accepted 8 October 1969.